Journal of Applied Geophysics 65 (2008) 111–120

Contents lists available at ScienceDirect

Journal of Applied Geophysics

journal homepage: www.elsevier.com/locate/jappgeo

High resolution 3D ERT to help GPR data interpretation for researching archaeological items in a geologically complex subsurface

S. Negri *, G. Leucci, F. Mazzone

Dipartimento di Scienza dei materiali, University of Lecce, Via Arnesano, 73100 Lecce, Italy

ARTICLE INFO

Article history:
Received 12 January 2007
Accepted 23 June 2008

Keywords:
3D ERT
ERT grid orientation effect
GPR
Messapian archaeological site

ABSTRACT

Muro Leccese (Lecce) contains one the most important Messapian archaeological sites in southern Italy.
The archaeological interest of the site arises from the discovery of the remains of Messapian walls, tombs, roads, etc. (4th–2nd centuries BC) in the neighbourhood. The archaeological remains were found at about 0.3 m depth. At present the site belongs to the municipality, which intends to build a new sewer network through it. The risk of destroying potentially interesting ancient archaeological structures during the works prompted an archaeological survey of the area. The relatively large dimensions of the area (almost 10,000 m^2), together with time and cost constraints, made it necessary to use geophysical investigations as a faster means to ascertain the presence of archaeological items. Since the most important targets were expected to be located at a soil depth of about 0.3 m, a ground-penetrating radar (GPR) survey was carried out in an area located near the archaeological excavations. Unfortunately the geological complexity did not allow an easy interpretation of the GPR data.
Therefore a 3D electrical resistivity tomography (ERT) scan was conducted in order to resolve these interpretation problems.
A three-way comparison of the results of the dense ERT measurements parallel to the *x* axis, the results of the measurements parallel to the *y* axis and the combined results was performed.
Subsequently the synthetic model approach was used to provide a better characterization of the resistivity anomalies visible on the ERT field data.
The 3D inversion results clearly illustrate the capability to resolve in view of quality 3D structures of archaeological interest. According to the presented data the inversion models along one direction (*x* or *y*) seems to be adequate in reconstructing the subsurface structures.
Naturally field data produce good quality reconstructions of the archaeological features only if the *x*-line and *y*-line measurements are considered together. Despite the increased computational time required by the 3D acquisition and 3D inversion schemes, good quality results can be produced.

Contents

1. Introduction

Electrical Resistivity Tomography (ERT) is widely used in the detection and investigation of shallow-depth targets. ERT has been applied with great success in solving problems of a geological (Griffiths and Barker, 1993; Leucci et al., 2004; Cardarelli and

* Corresponding author. Tel.: +39 0832297113; fax: +39 0832297100.
E-mail addresses: sergio.negri@unile.it (S. Negri), gianni.leucci@unile.it (G. Leucci), fiorella.mazzone@unile.it (F. Mazzone).

0926-9851/$ – see front matter © 2008 Elsevier B.V. All rights reserved.
doi:10.1016/j.jappgeo.2008.06.004

Fischanger, 2006), hydro-geological (Slater et al., 2002; Slater et al., 2003; Furman et al., 2004), environmental (Nowroozi et al., 1999; Van Schoor, 2002; Dahlin et al., 2002) and engineering (Brunner et al., 1999; Giannino et al., 2005; Godio et al., 2006) nature.

ERT is also very popular in archaeological investigations (Aspinall and Gaffney, 2001; Osella et al., 2005; De Domenico et al., 2006). The success of the method depends on the difference between the resistivity properties of the potential archaeological targets (walls, roads, buildings, etc) and the surrounding environment.

Over the past decade, significant progress has been made in the development of ERT field equipment and inversion programs. 3D ERT surveys have thus become more frequent. Because of their simplicity in terms of field implementation, 3D ERT surveys using sets of parallel 2D profiles are still used in most investigations. However, they can lead to misleading results in heterogeneous areas.

Several studies have looked at survey designs and layout strategies that yield optimum information using different ERT survey configurations or set up in different geological settings.

Loke and Barker (1996) used 3D ERT with a pole-pole array to obtain images of sand channels in a 3×3 m block. They conclude that in this situation 2D ERT surveys are probably not adequate to properly scan the subsurface. Chambers et al. (2002) used orthogonal sets of dipole–dipole and Wenner 2D lines to scan known targets at an experimental site. They conclude that 3D inversions are superior to quasi-3D images produced from sets of 2D inversions. Bentley and Gharibi (2004) used sets of orthogonal 2D ERT survey lines in a geometrically complex heterogeneous decommissioned gas plant. They demonstrated distortions in 2D images and concluded that appropriately designed 3D arrays can be used efficiently for site characterization. Recently Papadopoulos et al. (2006) used 3D pole–pole data collected from archaeological areas. They investigated the effectiveness of 2D and 3D non-linear inversion algorithms in the processing and interpretation of ERT data using both synthetic and real data. They conclude that the reconstructed 3D images do not suffer from the visual artefacts encountered in the quasi-3D approach, owing to the 3D nature of the archaeological features.

In this paper the authors focused on a methodological approach that allow to use a quasi 3D ERT acquisition and processing if a preliminary GPR survey has been performed. Results demonstrate it is possible to obtain high resolution geophysical imaging using a quasi-3D ERT grid with parallel profile 1 m spaced and inter-electrodes distance by 1 m. In this way the archaeological target could be well resolved in a geologically complex contest.

GPR data give useful information about the target orientation and helped the ERT survey designed. The knowledge of target orientation allow to acquire ERT data in only one direction and therefore reduces the survey costs and the time of acquisition and elaboration of data without to compromise the results.

2. Site description

Muro Leccese is in the province of Lecce, in the Salento peninsular (South Italy). It is located about 40 km southeast of Lecce (Fig. 1).

Muro Leccese partly overlaps an ancient Messapian settlement, whose name is unknown. The most ancient archaeological evidence (8th–7th centuries BC) is related to a native community living in scattered nuclei of huts. In the 4th century BC the inhabited area took on an urban character, with houses built along the roads. A wall built of square blocks, 4 km long, encloses an area of about 100 ha. In the 3rd century BC the inhabited area shrank drastically, probably as a result of the conflict with Rome.

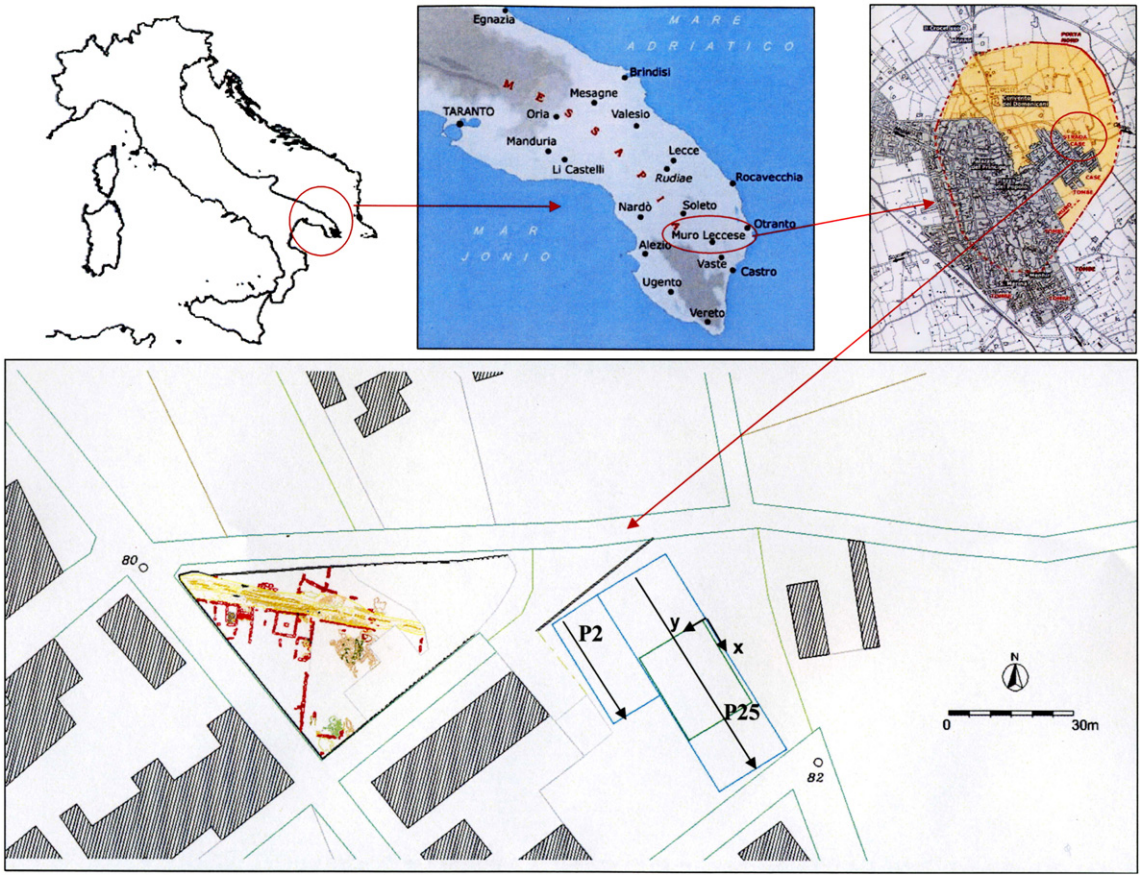

Fig. 1. The archaeological site of Muro Leccese (Lecce, Italy): location of surveyed area map.

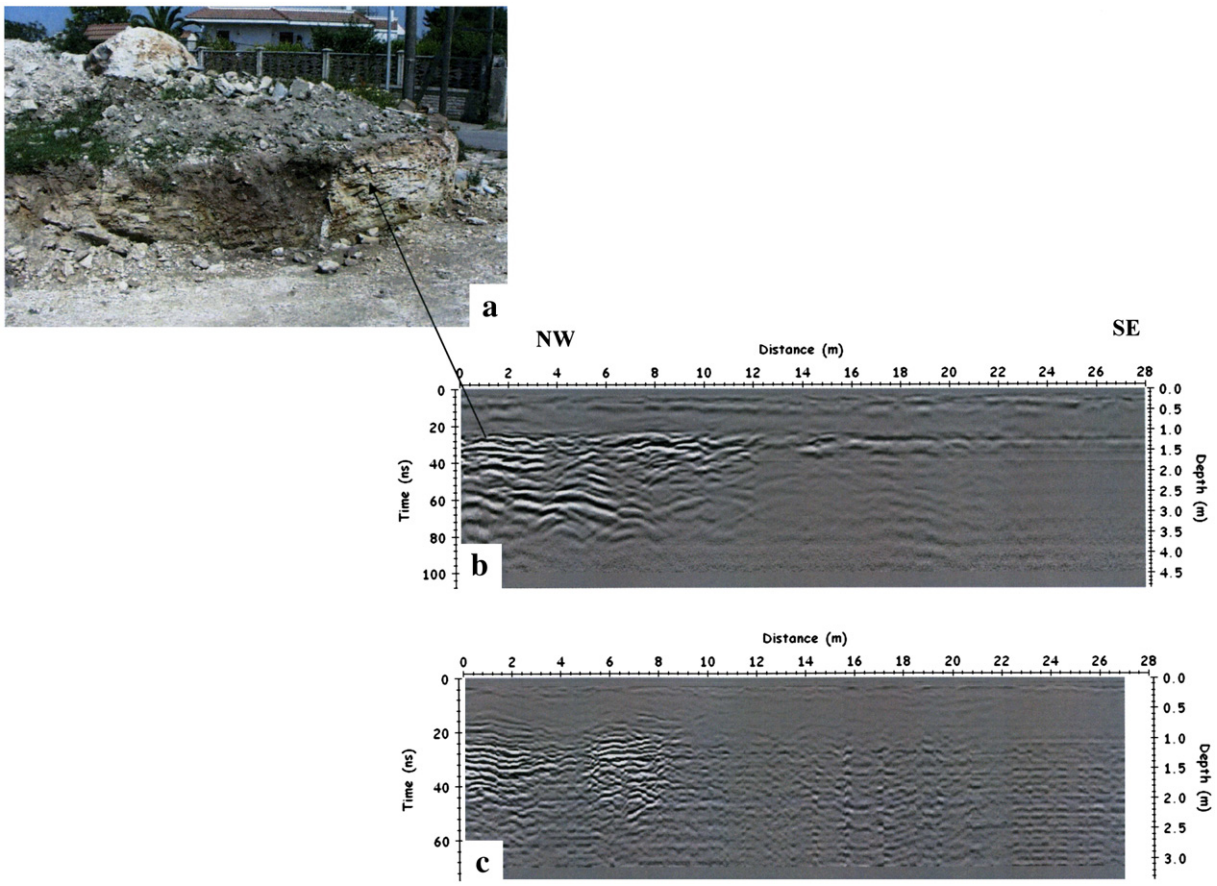

Fig. 2. The GPR survey: a) Photo of the alternation of simply folded marne and calcarenite in the substrate, which outcrops in where the road runs past the surveyed area; b) 200 MHz antenna processed radar section related to the P2 profile; c) 500 MHz antenna processed radar section related to the P2 profile.

The Messapian settlement of Muro has not been systematically explored, but for many decades has suffered a new "destruction" in the form of continuous building. The acquisition of some areas containing archaeological remains and the drawing up in 1999 of an agreement between the Municipality, the Archaeological Protection Authority ("Sovraintendenza") and the Department of Cultural Heritage of the University of Lecce, laid the ground for a new approach to the archaeological exploration of some sectors of the Messapian settlement. In 2001, archaeologists from the University of Lecce started to survey a Messapian residential district of the 4th century BC), situated to the East of the modern inhabited area known as "Cunella".

The results of these initial explorations were a village composed of groups of huts at some distance from each other, occupying the highest points of the territory. These huts were of circular or oval form; the lower walls were built of stone and the upper walls of clay and wood, with a roof of straw and clay (Giardino, 2002; Guastali, 2003).

Data from the archaeological excavations and geological observations (box core samples) made it possible to reconstruct the stratigraphy of the first ten metres of sediments. About 0.3 m of covering materials (such as agricultural terrain) rest on the surface. Beneath this lies a calcarenite layer of up to 5 m in depth. In places, this calcarenite is covered by up to three metres of alternating marne and clay deposits (Margiotta, personal communication).

3. The previous GPR survey

The evidence of the partial overlap of the modern village with the ancient inhabited area, as well as the threat from building expansion, prompted the municipal authorities to identify, as a matter of urgency, the areas where building activities would need to be prohibited in order to safeguard the buried archaeological heritage and recover it for appreciation by the public.

The GPR survey at the archaeological site of Muro was carried out using a Sir-2 digital pulse radar system made by GSSI (Geophysical Survey System Inc.) with both 200 and 500 MHz centre-frequency antennas. The survey was carried out in an area (Fig. 1), located on the East side of the excavation site (Carrozzo et al., 2002).

Given the shallow depth of the structures of interest and the high resolution required, few profiles were performed using the 200 MHz antenna; most of the GPR survey was carried out using the 500 MHz antenna along parallel profiles 0.5 m apart (Fig. 1) with a NW–SE orientation. The acquisition parameters (time window, gain function, filters) were kept constant for all the profiles acquired so as to facilitate comparison and ensure that the data were as homogeneous as possible.

The processing of the GPR data consists essentially of the following steps:

- trace editing and normalization of the horizontal scale sampling intervals of 0.025 m;
- reconstruction of the saturated wave form ('declipping');
- filtering of background by removing the average trace;
- manual application of a time-variant gain function;
- application of band-pass filters;
- Estimation of the average velocity of propagation using the diffraction hyperbola method;
- Kirchhoff 2D migration using the previously estimated velocity values (roughly 9.0 cm/ns);
- construction of the time slices using appropriate time windows (Conyers and Goodman, 1997).

Despite the effects of system ringing and the jogging of the antenna as it moved across the ground surface, it was possible to

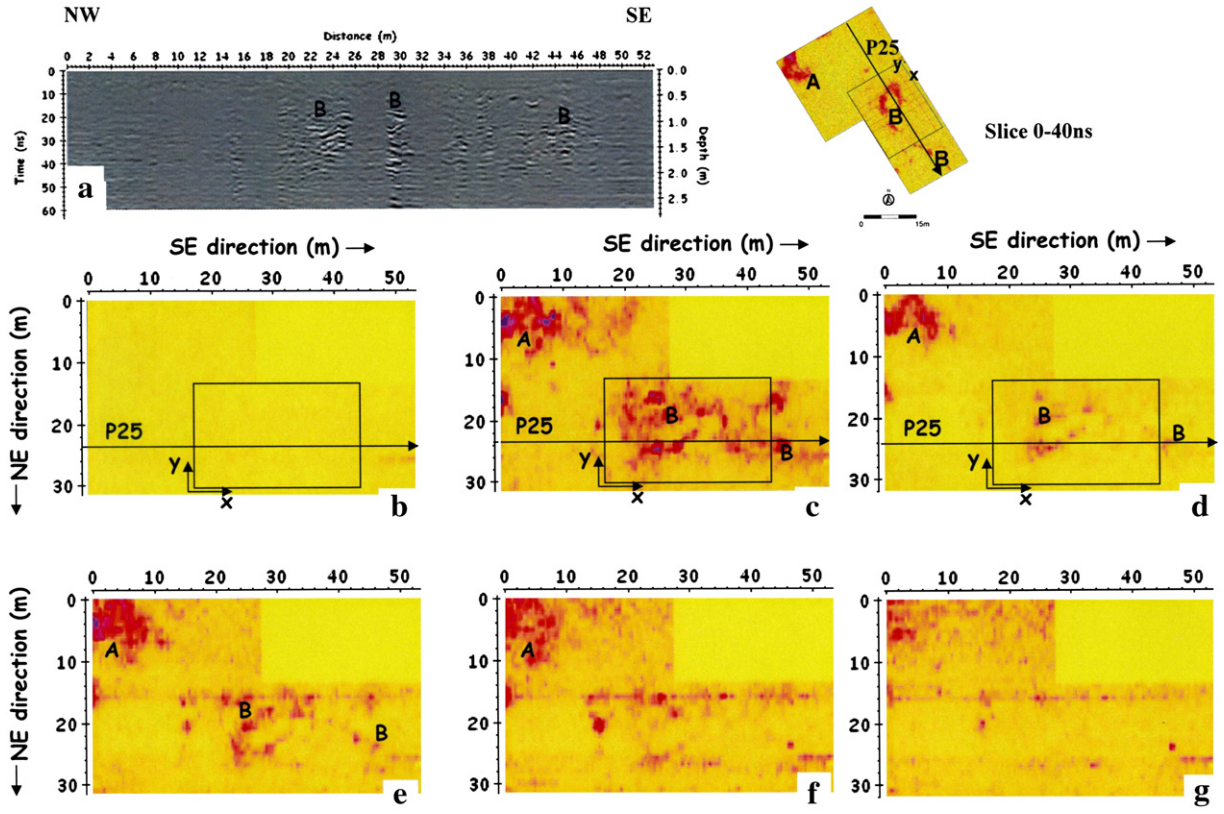

Fig. 3. The GPR survey: a) 500 MHz antenna processed radar section related to the P25 profile; b) time slice 0–10 ns; c) time slice 10–20 ns; d) time slice 20–30 ns; e) time slice 30–40 ns; f) time slice 40–50 ns; g) time slice 50–60 ns.

recognise a useful signal in the radar profiles acquired. In large parts of the area however, the signal was very weak, perhaps due to a greater thickness of the topsoil, and the depth of penetration was considerably reduced. Particularly intense continuous reflections were present up to roughly 50 ns (Fig. 2b and c) in the NW corner of the area (Fig. 1). These were due to the alternation of simply folded marne and calcarenite in the substrate, which outcrops in where the road runs past the surveyed area (Fig. 2a). The photograph shows the presence of "terra rossa" and heterogeneous material (deriving from both karstic dissolution and anthropogenic activities), of higher conductivity, used to fill in the cavities.

Less intense and more discontinuous reflections were detected in the same time window in the profiles acquired in the central part of the area. These reflections are characterized by sharp interruptions, for example between 29 and 32 m on the profile shown in Fig. 3a, where the absorption of the signal suggests a thickening in that point of the (more conductive) layer of topsoil. These brusque lateral variations may attributed either to natural phenomena deriving from the karstic nature of the terrain, or to some anthropogenic origin.

Using the time slice construction technique (Conyers and Goodman, 1997) and employing the GPR data within six time windows 0–10 ns a planimetric representation of the radar energy in the first 2.70 m of depth (Fig. 3b–g) was drawn up. In the central part of the area and in the time slices 10–20 ns, 20–30 ns and 30–40 ns (Fig. 3c,d,e) a high-intensity pseudo-elliptical zone, labelled B, can be seen.

Some strong radar anomalies (labelled A) were also detected in the North-west corner near the road. These have been interpreted as resulting from the fractured and karstified bedrock together with the infill material mentioned above. However, the question of how to interpret the roughly elliptical shallow anomaly B — specifically, whether it is likely to be of archaeological interest, remains to be resolved.

To resolve this question, in October 2002 the 3D ERT survey was performed.

4. The field ERT data

A 3D survey was conducted at the archaeological site of Muro Leccese. The area surveyed, measuring 23 m by 18 m, was selected so as to cover the elliptical shallow anomaly (B) detected in the GPR survey (Fig. 3b). The survey entailed a set of 19 dipole–dipole lines in the x direction, each with 24 electrodes, and a perpendicular set of 24 dipole–dipole lines in the y direction, each with 19 electrodes. In both directions the lines were spaced 1 m apart, and the distance between electrodes along the lines was also 1 m. The chose of lines spacing and electrodes distance was due to the GPR survey results that evidenced anomalous zone with dimension of some meters (Fig. 3). The dipole *a* spacing varied from 1 to 2 m. The maximum distance between the current pair and potential pair of electrodes was limited to a maximum of $n=6$ *a*-spacings. Larger interdipole spacings led to unacceptable levels of noise in the data. A Syscal R1 (Iris-Instruments) resistivity meter was used. A total of 5741 data points were measured and the results of the joint 3D inversion of the data sets from the *x*, *y* and *xy* directions were considered. The acquired data were combined to produce three-dimensional depth slices of the resistivity distribution in the *x*, *y* and *xy* directions.

Resistivity data were inverted with the RES3DINV program (Loke and Barker, 1996). The inversion program uses a block model in which resistivity values are assigned in the prisms within a 3D mesh. The program attempts to achieve convergence between apparent resistivity values and calculated model by using the smoothness constrained least square method (deGroot-Hedlin and Constable, 1990; Sasaki, 1992; Loke and Barker, 1996), in which the Jacobian matrix is calculated after each inversion. The finite-difference method

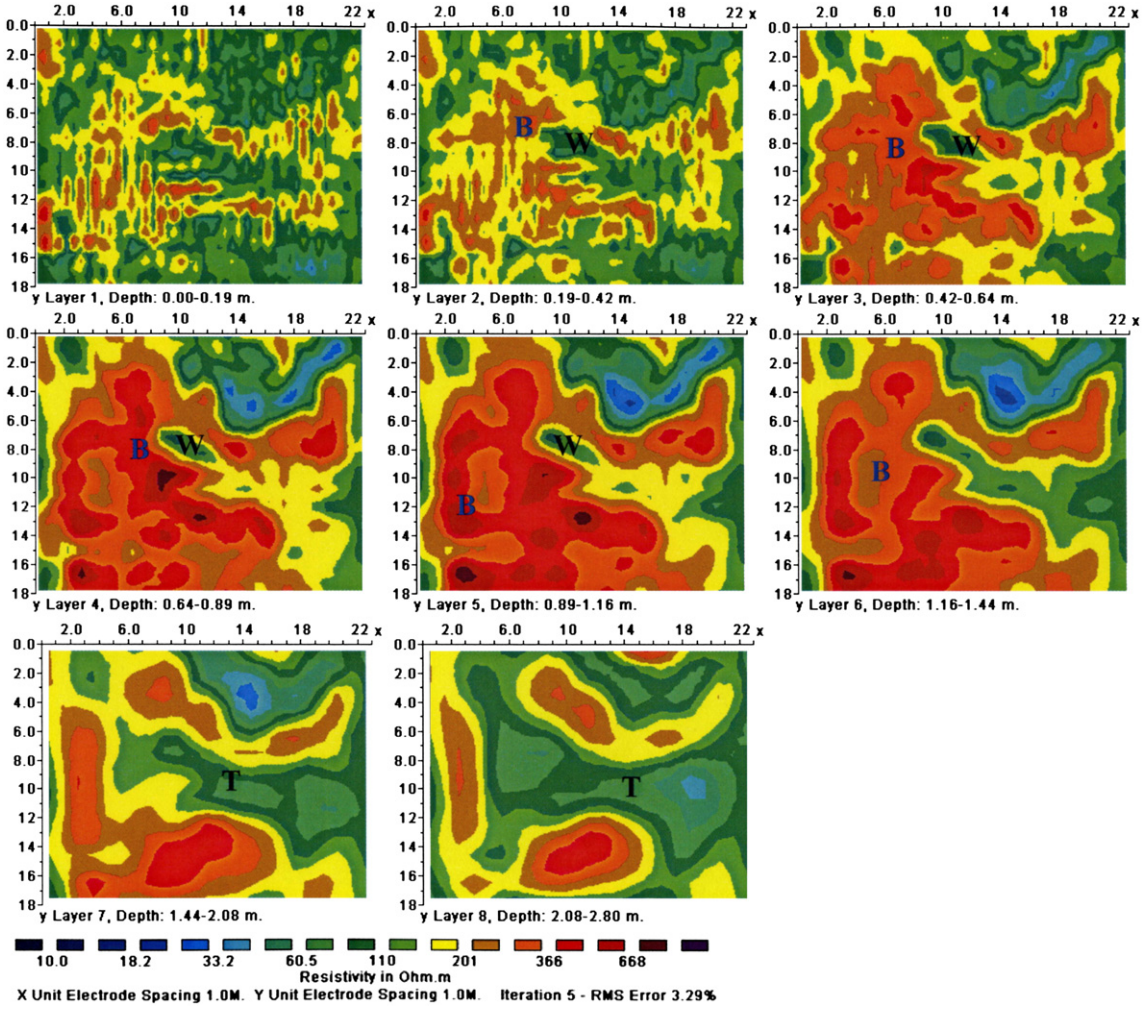

Fig. 4. ERT survey: depth slices of increasing depth that resulted from the 3D inversion of the *x* oriented data.

was applied in order to calculate forward response of the geoelectrical models while Gauss–Newton optimization method was used to solve the inverse resistivity problem. The blocks were divided in half, vertically and horizontally, in order to provide better resolution of the calculated resistivity distribution, but the results have show that there are not more difference between the resistivity models obtained using the option with the blocks divided in half, vertically and horizontally and the models obtained without this option. It is probably due to the lines spacing and electrodes distance that are comparable with the target dimensions.

A RMS errors of 3.29% for *x* direction, 4.26% for *y* direction, and 3.69% for *xy* direction data sets were achieved after 5 iterations. Increasing the number of iterations the RMS error doesn't vary significantly.

Figs. 4, 5 and 6 show the eight slices of increasing depth that resulted from the 3D inversion of the *x*, *y* and *xy* data respectively.

An elliptical shallow anomaly (labelled B) of high resistivity (greater 400 Ωm) appears in the 0.19,…, 2.08 m, depth slices of the *x*, *y* and *xy* direction data inversions.

This anomaly confirms the elliptical shallow anomaly (B) detected by the GPR survey (Fig. 3b).

Due to its high resistivity values, typical of Salento calcarenite (Leucci et al., 2004), anomaly B has been interpreted as a section of the calcarenite bedrock in which an elliptical hollow was excavated. The nature of this anomaly is suggestive due to the *low* resistivity values (ranging from 100 to 150 Ωm, labelled w in Figs. 4, 5 and 6) of the materials contained inside it. The anomaly W, visible inside anomaly B, in the 0.19,…, 1.16 m depth slices, may be a feature of archaeological interest.

In the 1.16,…, 2.80 m deeper slices, below the anomaly W, the resistivity values decrease until to about 40 Ωm. This lower resistivity zone, labelled T, could represent once more a stratigraphic level inside the calcarenite bedrock that may be of archaeological interest.

The 3D images reconstructed from the *x*, *y* and *xy* direction surveys are similar but not identical to each other. The W and T anomalies appear to have a different shape depending on the direction of acquisition.

Subsequent archaeological excavations performed in the area where anomaly B was found have confirmed the existence of a little pebble wall (0.2–0.9 m in depth) and a series of tombs (about 1.7 m in depth) (Fig. 7).

Particularly the excavation stratigraphy (Fig. 8a) includes a thin 0.40 m ground layer and an underlying pebbles layer (0.40–0.90 in depth). From about 0.90 m to about 1.7 m in depth is a layer with ground and pebble. At about 1.70 m in depth are the tombs. The tombs were found filled with ground. Centered at 0.20 m in depth on the centre part of the excavation is a wall of pebbles.

Lines E8*x* (Fig. 8b) and E12*y* (Fig. 8c) were imaged and compared with the archaeological excavation results. Electrical resistivity values greater 400 Ωm are related to the calcarenite bedrock. The resistivity model related to the E8*x* line (Fig. 8b) show the presence of a little

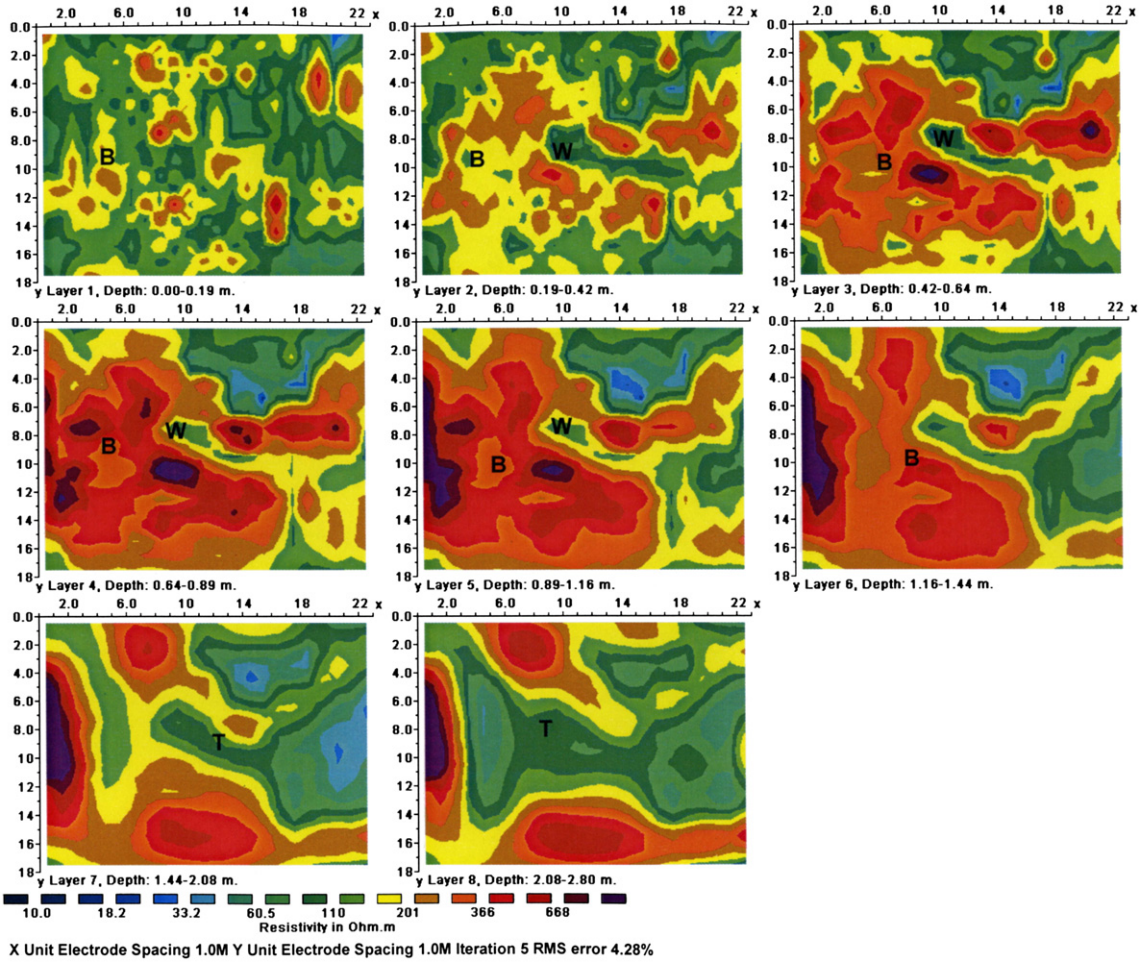

Fig. 5. ERT survey: depth slices of increasing depth that resulted from the 3D inversion of the y oriented data.

anomaly (about 100 Ωm) between approximately x=9.5 m and x=11.0 m. In these points the E8x line go through the wall of pebbles which the archaeologists found after the excavation (Fig. 8a). In the resistivity model shows in Fig. 8b is clearly visible the layer filled with pebbles. In this layer the resistivity values increase from 60 to about 200 Ωm. An high resistivity zone (about 200–300 Ωm) between approximately 0.9 m and 1.7 m in depth is clearly visible and could be related to the layer composed by ground and pebbles. Below this layer the tombs were found.

The resistivity model related to the E12y line (Fig. 8c) show the presence of a low resistivity zone (70–110 Ωm) between approximately y=7.5 m and y=9.5 m. In this zone a cut in the calcarenite bedrock was found.

Subsequently the x, y and xy ERT data sets were compared with the results of these archaeological excavations in order to evaluate their utility in eliminating the intrinsic ambiguity related to the shape of the W and T anomalies.

Figs. 9, 10, and 11 show the superimposition of the archaeological features discovered (wall and tombs) on the resistivity model depth layers obtained from the data sets for the x (Fig. 9), y (Fig. 10), and xy (Fig. 11) directions.

The comparison confirms that the depth slices were able to reconstruct the three-dimensional feature reasonably well but that there are some differences between the results obtained from the x, y and xy data.

The 3D inversion models (x, y, xy) show comparable accuracy (Figs. 9, 10 and 11). Although some minor differences can be observed in the major features (W and T). The W feature was well defined in the x, and xy direction because the W feature was almost oriented in the x direction (Figs. 9 and 11). The T anomaly was resolved with comparable accuracy in the x, y, and xy inversion models respectively (Fig. 9, 10 and 11). It is due to de dimension of T anomaly (about 2×2 m) that are greater than lines spacing and electrodes distance.

5. Synthetic ERT data

Synthetic data were created in order to understand the complexity of the subsoil condition and therefore to help in interpretation of field data.

The synthetic data were created by assuming a 2D resistivity model (Fig. 12a) that includes a 800 Ωm surface layer (1.50 m thickness) A and an underlying 30 Ωm layer (1.25 m thickness) B. Layer A appears again below layer B. These layers could correspond to a calcarenite bedrock (A) overlying a conductive ground (B) and again the calcarenite bedrock (A). At the 11.5 m in the x direction, a rectangular block (W) with a resistivity of 400 Ωm is cetered. The block is located inside a rectangular conductivity material (30 Ωm). Block W represent the wall of pebble, found inside a ground material, after the archaeological excavation.

In Fig. 12c the 2D resistivity model was created in order to simulate the cut inside the calcarenite bedrock without the wall of pebble.

To simulate the performed field survey, 24 electrodes are spread across the top of the model at regular 1 m intervals. The dipole–dipole array was used.

The synthetic data were generated with Res2Dmod software (Loke, 2001). The 2-D model was created using the finite-difference method

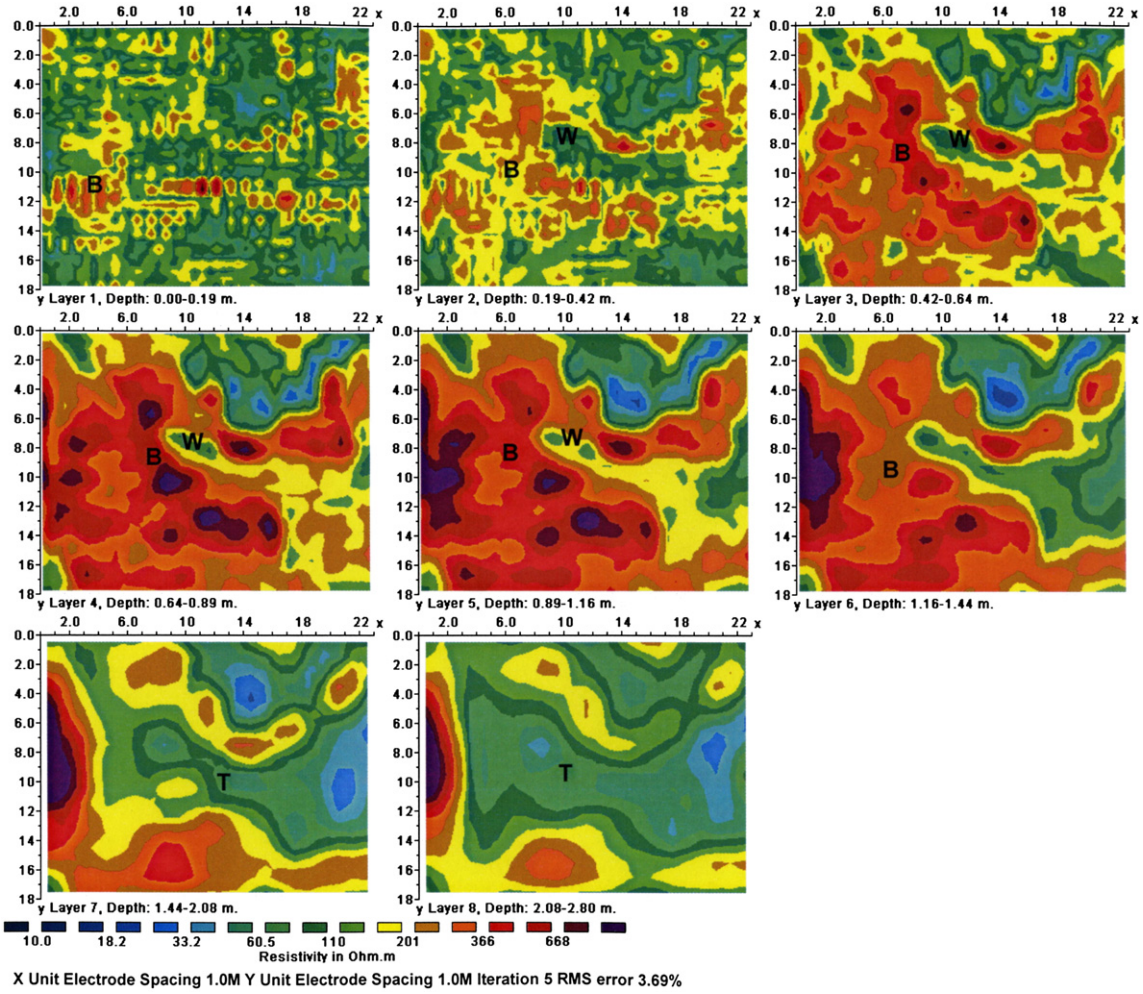

Fig. 6. ERT survey: depth slices of increasing depth that resulted from the 3D inversion of the *xy* oriented data.

that divides the subsurface into a number of blocks using a rectangular mesh (Dey and Morrison, 1979; Loke 1994).

Subsequently, the inversion procedure for the data sets was completed after 5 iterations using the Res2Dinv software (Loke, 2004).

The Gauss–Newton and finite-difference option was used. The model cells with widths of half the unit spacing option was used in order to provide better resolution of the calculated resistivity distribution. A RMS errors of about 5% was achieved after 5 iterations. Increasing the number of iterations the RMS error doesn't vary significantly.

Fig. 12b and d show the resistivity images determined from the resistivity model showed in the Fig. 12a and c respectively.

The observation of the results indicates that the wall should be quite well resolved.

Subsequently the 2D ERT field data were compared with the synthetic data. Particularly the E8*x* line (Fig. 12e) was considered. In fact E8*x* line goes through the wall of pebbles which the archaeologists found after the excavation.

When compared the Fig. 12b and e demonstrate that the anomaly W could be interpreted as wall.

6. Conclusions

The question that arises in cases such as these concerns the optimum survey technique; one way to map the archaeological features with a good resolution would be to conduct a full 3D ERT survey, but full 3D ERT measurements are very time-consuming.

The field data showed that resistivity inversion models along the *x*, *y*, and *xy* direction respectively can delineate the subsurface structure with comparable accuracy if the lines spacing and electrodes distance are comparable with the target dimension, but if the orientation of archaeological feature is unknown, only the combination of an *xy* survey yielded satisfactory results.

In the examples presented in this paper, the results from the inversion of field data where the archaeological feature had low resistivity in comparison to its background showed that the grid orientation effect was absent in the *x* and *xy* data sets, thus successful in resolving the anomaly even when a single set of parallel profiles was used. However, these results depend also on the target orientation in respect the grid orientation.

Furthermore we emphasize the utility of both 2D GPR and ERT field data. Particularly the 2D ERT data (field together synthetic data) allowed a better interpretation of anomalies zone (stratigraphy and wall of pebbles).

Using synthetic data we assessed the imaging potential of data acquired in the field.

To summarise, ERT data help to resolve the ambiguities in the interpretation of GPR data. Furthermore, the option in ERT data processing in which the blocks were divided in half, vertically and horizontally provides a resolution comparable with ERT data

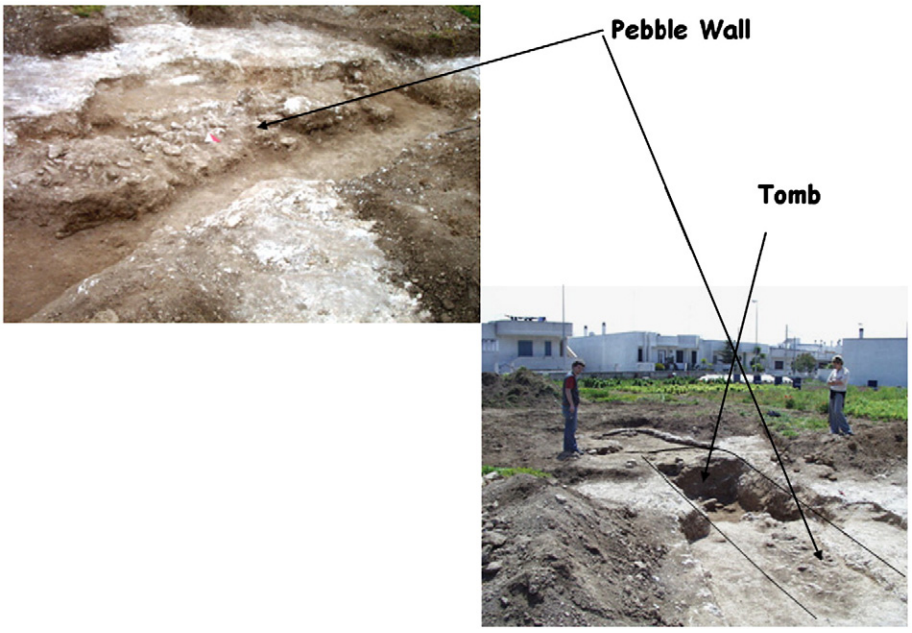

Fig. 7. The archaeological site of Muro Leccese (Lecce, Italy): photos of the tomb and wall found after the geophysical investigations.

processing in which the blocks were not divided. It is probably due to the lines spacing and electrodes distance that are comparable with the target dimensions.

Is important to underling that the GPR data give useful information about the target orientation and dimension and helped to design the ERT survey. In fact the knowledge of target orientation and dimension allow both to acquire ERT data in only one direction, to determine the lines spacing and electrodes distance, and therefore reduces the survey costs and the time of acquisition and elaboration of data.

Acknowledgements

This work was made possible thanks to the cooperation of Prof. Liliana Giardino, professor of "Classical Urban Studies" at the Department of Cultural Heritage at the University of Lecce (Italy).

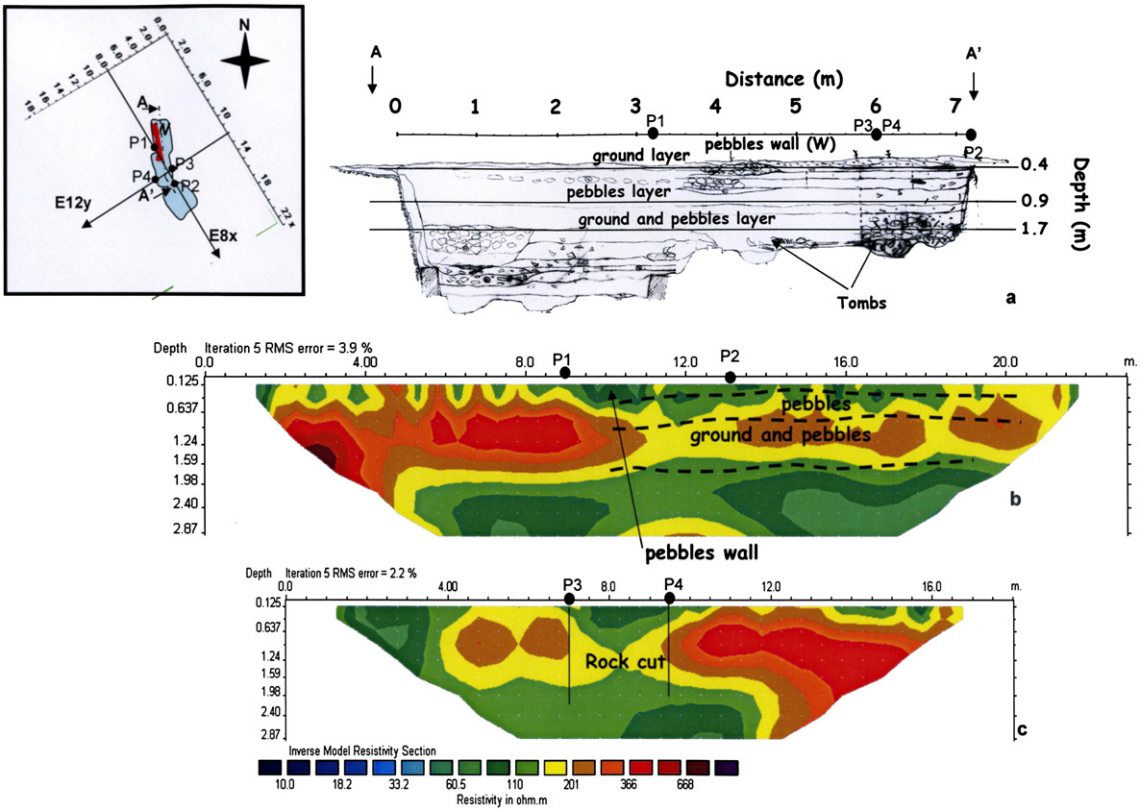

Fig. 8. Comparison between a) the archaeological remains location and the ERT 2D resistivity distribution in subsoil — b)E8*x*, c) E12*y*.

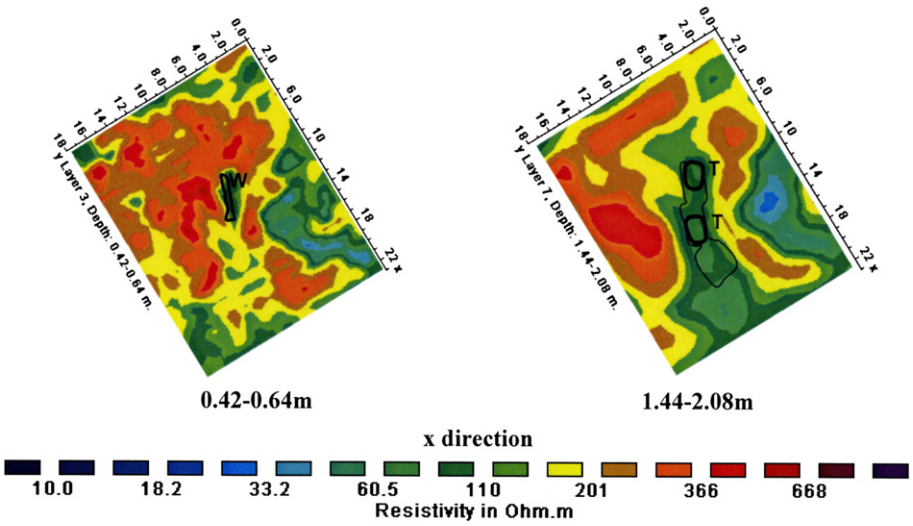

Fig. 9. Comparison between the ERT depth slices (*x*-direction) and the archaeological remains location.

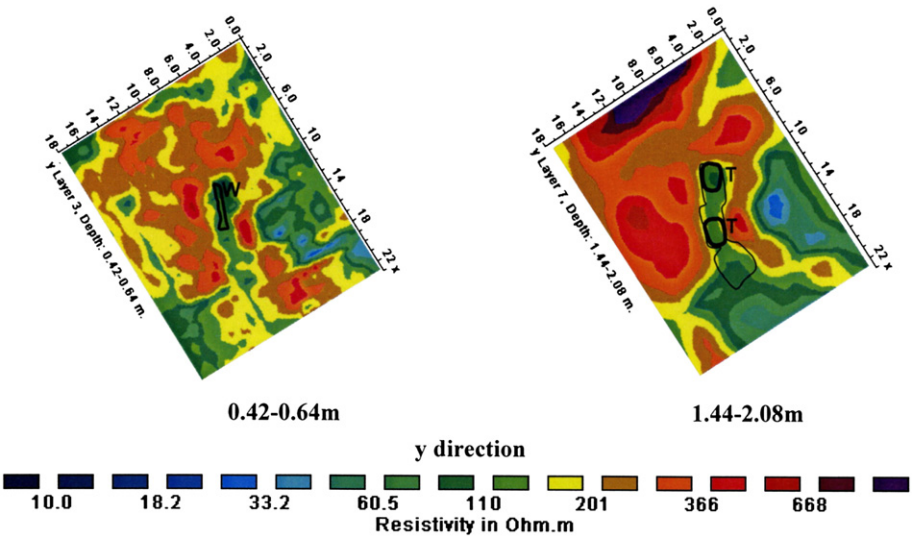

Fig. 10. Comparison between the ERT depth slices (*y*-direction) and the archaeological remains location.

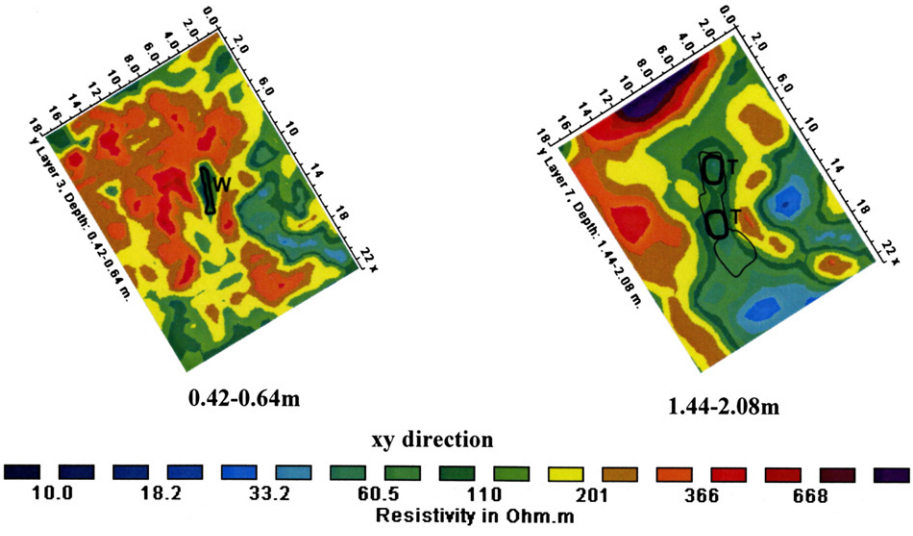

Fig. 11. Comparison between the ERT depth slices (*xy*-direction) and the archaeological remains location.

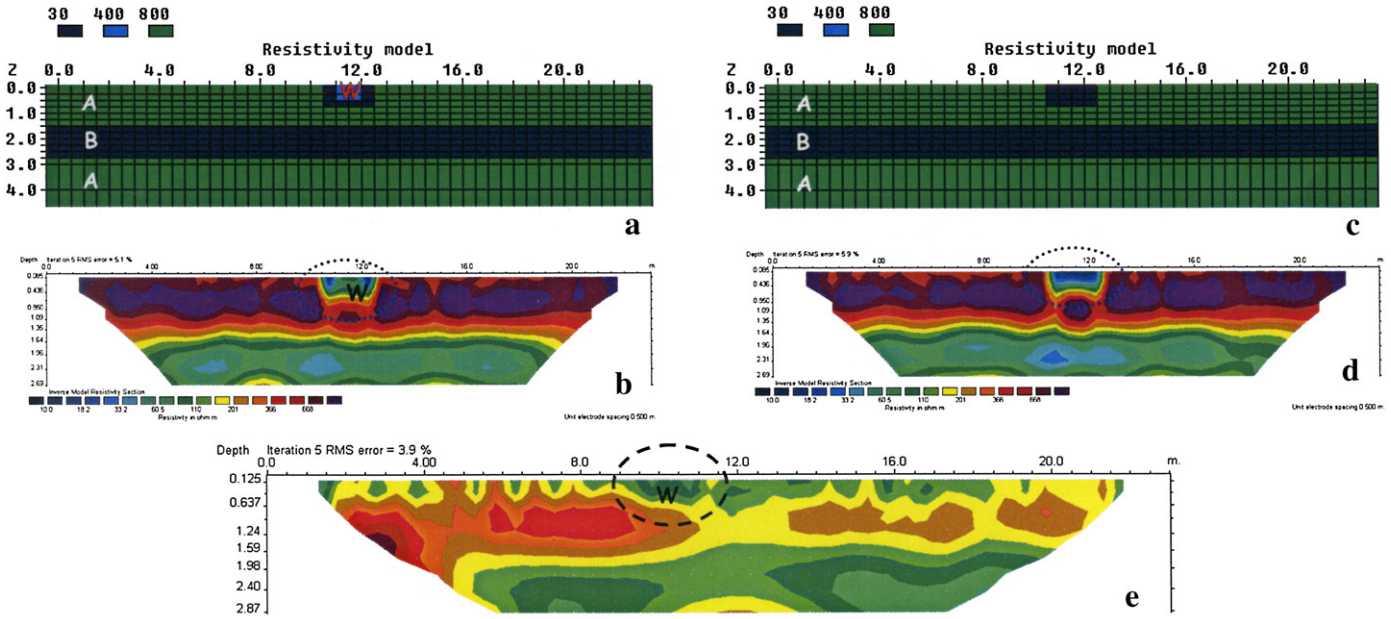

Fig. 12. Resistivity model employed for the analysis of field data: a) with wall; b) result of the inversion with the wall; c) without wall; d) result of the inversion without the wall; e) the field data related to E8*x* line.

The authors would like to thank also Dr. Catia Bianco for the documentation and archaeological maps.

References

Aspinall, A., Gaffney, C.F., 2001. The Schlumberger array-potential and pitfalls in archaeological prospection. Archaeological Prospection 8, 199–209.

Bentley, L.R., Gharibi, M., 2004. Two and three-dimensional electrical resistivity imaging at a heterogeneous remediation site. Geophysics 69, 674–680.

Brunner, I., Friedel, S., Jacobs, F., Danckwardt, E., 1999. Investigation of a Tertiary maar structure using three-dimensional resistivity imaging. Geophysical Journal International 136, 771–780.

Cardarelli, E., Fischanger, F., 2006. 2D data modelling by electrical resistivity tomography for complex subsurface geology. Geophysical Prospecting 54, 121–133.

Carrozzo, M.T., Leucci, G., Negri, S., Nuzzo, L., 2002. Applicazione di metodi elettrici, magnetici ed elettromagnetici per prospezioni archeologiche in area urbana: il caso di Muro Leccese (Lecce). Atti del 21° Convegno Nazionale GNGTS, Roma 6–9 Novembre 2002.

Chambers, J.E., Ogilvy, R.D., Kuras, O., Cripps, J.C., Meldrum, P.I., 2002. 3D electrical imaging of known targets at a controlled environmental test site. Environmental Geology 41, 690–704.

Conyers, L.B., Goodman, D., 1997. Ground-Penetrating Radar — An introduction for archaeologists. AltaMira Press. 232 pp.

Dahlin, T., Bernstone, C., Loke, M.H., 2002. A 3-D resistivity investigation of a contaminated site at Lernacken, Sweden. Geophysics 67, 1692–1700.

De Domenico, D., Giannino, F., Leucci, G., Bottari, C., 2006. Integrated geophysical surveys at the archaeological site of Tindari (Sicily, Italy). Journal of Archaeological Science 33, 961–970.

deGroot-Hedlin, C., Constable, S., 1990. Occam's inversion to generate smooth, the dimensional models from magnetotelluric data. Geophysics 55, 1613–1624.

Dey, A., Morrison, H.F., 1979. Resistivity modelling for arbitrary shaped two dimensional structures. Geophysical Prospecting, 27, 1020–1036.

Furman, A., Ferré, T.P.A., and Warrick, A.W. 2004. Optimization of ERT surveys for monitoring transient hydrological events using perturbation sensitivity and genetic algorithms. Available at www.vadosezonejournal.org. Vadose Zone J. 3:1230–1239.

Giannino, F., Leucci, G., Teramo, A., De Domenico, D., 2005. Geophysical surveys to improve the knowledge on the S. Salvatore fortress structure (Messina, Italy). Atti del 24° Convegno Nazionale del GNGTS; Roma 15, 16 e 17 Novembre 2005. CD-Rom.

Giardino, L., 2002. Muro Leccese. La città messapica senza nome: dal libro di Pasquale Maggiulli 1992 al parco archeologico del 2000. Edizioni Goffreda, Maglie (Lecce).

Godio, A., Strobbia, C., De Bacco, G., 2006. Geophysical characterisation of a rockslide in an alpine region. Engineering Geology 83, 273–286.

Griffiths, D.H., Barker, R.D., 1993. Two-dimensional resistivity imaging and modelling in areas of complex geology. Journal of Applied Geophysics 29, 211–226.

Guastali, M., 2003. Lo sguardo di Icaro. Le collezioni dell'Aereofototeca Nazionale per la conoscenza del territorio, pp. 336–338. Edizioni Campisano.

Leucci, G., Margiotta, S., Negri, S., 2004. Geological and geophysical investigations in karstic environment (Salice Salentino, Lecce, Italy). Journal of Environmental and Engineering Geophysics (JEEG) 9, 25–34.

Loke, M.H., , 1994, The inversion of two-dimensional apparent resistivity data. unpubl. Ph.D. thesis, Un. of Birmingham (U.K.).

Loke, M.H., 2001. Res2DMod ver. 3.02a. Geotomo Software. www.geoelectrical.com.

Loke, M.H., 2004. Res3Dinv ver 2.14. Geotomo Software. www.geoelectrical.com.

Loke, M.H., Barker, R.D., 1996. Practical techniques for 3D resistivity surveys and data inversion. Geophysical Prospecting 44, 499–523.

Nowroozi, A.A., Horrocks, S.B., Henderson, B., 1999. Saltwater intrusion into the freshwater aquifer in the eastern shore of Virginia: a reconnaissance electrical resistivity survey. Journal of Applied Geophysics 42, 1–22.

Osella, A., de la Vega, M., Lascano, E., 2005. 3D electrical imaging of an archaeological site using electrical and electromagnetic methods. Geophysics 4, 101–107.

Papadopoulos, N.G., Tsourlos, P., Tsokas, G.N., Sarris, A., 2006. Two-dimensional and Three-dimensional resistivity Imaging in Archaeological Site Investigation. Archaeological Prospection 13, 75–90.

Sasaki, Y., 1992. Resolution of resistivity tomography inferred from numerical simulation. Geophysical Prospecting 40, 453–464.

Slater, L., Glaser, D., Utne, J.I., Binley, A., 2002. Electrical imaging of permeable reactive barrier integrity. Proceedings of the Symposium on the Application of Geophysics to Environmental & Engineering Problems (SAGEEP), February 10–14, Las Vegas, NE, 10pp.

Slater, L., Binley, A., Reeve, A., 2003. Solute transport processes in peat inferred from electrical imaging. Proceedings of the Symposium on the Application of Geophysics to Environmental & Engineering Problems (SAGEEP2003), April, San Antonio, TX, pp. 676–686.

Van Schoor, A., 2002. Detection of sinkholes using 2D electrical resistivity imaging. Journal of Applied Geophysics 50, 393–399.